EUROPEAN ORGANIZATION FOR NUCLEAR RESEARCH

Proposal to the ISOLDE and Neutron Time-of-Flight Committee

Charge radii and moments of $^{47-51}$Sc, crossing $N = 28$, measured with bunched beam collinear laser spectroscopy at COLLAPS

October 19, 2015

X.F. Yang[1], M.L. Bissell[2], K. Blaum[3], B. Cheal[4], S. Ettenauer[5], K.T. Flanagan[2], R.F. Garcia Ruiz[2], W. Gins[1], C. Gorges[6], H. Heylen[1], S. Kaufmann[6], Á. Koszorús[1], J. Krämer[6], M. Kowalska[5], K.M. Lynch[5], G. Neyens[1], R. Neugart[3,7], W. Nörtershäuser[6], R. Sánchez[8], S.G. Wilkins[2], D.T. Yordanov[9].

[1] *KU Leuven, Instituut voor Kern- en Stralingsfysica, B-3001 Leuven, Belgium*
[2] *School of Physics and Astronomy, The University of Manchester, Manchester, M13 9PL, UK*
[3] *Max-Plank-Institut für Kernphysik, D-69117 Heidelberg, Germany*
[4] *Oliver Lodge Laboratory, Oxford Street, University of Liverpool, L69 7ZE, United Kingdom*
[5] *Physics Department, CERN, CH-1211 Geneva 23, Switzerland*
[6] *Institut für Kernphysik, TU Darmstadt, D-64289 Darmstadt, Germany*
[7] *Institut für Kernchemie, Universität Mainz, D-55128 Mainz, Germany*
[8] *GSI Helmholtzzentrum für Schwerionenforschung, D-64291 Darmstadt, Germany*
[9] *Institut de Physique Nucléaire Orsay, IN2P3/CNRS, 91405 Orsay Cedex, France*

Spokesperson: Xiaofei Yang [xiaofei.yang@fys.kuleuven.be]
Contact person: Ronald Fernando Garcia Ruiz [ronald.fernando.garcia.ruiz@cern.ch]

CERN-INTC-2015-050 / INTC-P-450
19/10/2015

Abstract:
To obtain a global understanding of the evolution of nuclear structure in the Ca region, experimental efforts in collinear laser spectroscopy have been dedicated to the K ($Z = 19$) and Ca ($Z = 20$) isotopic chain in the last few years [8-12]. As a continuation of these studies, we propose to measure the moments and mean-square charge radii of $^{47-51}$Sc. The measurements will cross the $N = 28$ shell closure and constitute a prominent test of state-of-the-art theoretical calculations developed in the Ca region.

Requested shifts: [12] shifts of radioactive beam.

1 Introduction

The calcium isotopic chain, with a magic proton number ($Z = 20$) and two neutron closed shells ($N = 20, 28$) has always been of great interest for both theoretical and experimental studies [1-5]. Especially, the attention has been recently focused on the nuclear structure evolution beyond $N = 28$ because of two newly suggested neutron closed shells ($N = 32, 34$) [3-7]. The proposed new magic numbers have attracted a lot of experimental and theoretical studies in the Ca region. Numerous experimental efforts have been dedicated to the measurement of ground-state properties, such as the masses, spins, electromagnetic moments and charge radii, in both K ($Z = 19$) and Ca ($Z = 20$) isotopes using different experimental techniques [8-13]. Naturally, the next experimental focus in this region comes to the Sc isotopic chain, with one valence proton in the $\pi f_{7/2}$ orbit above the $Z = 20$ closed shell. High-precision mass measurements have been recently proposed [14], and some collinear laser spectroscopy measurements were performed already on the less exotic Sc isotopes at Jyväskylä [15].

In the mean time, many theoretical tools have been developed to describe the nuclear structure properties in this region. The most extensively used two body effective interactions are the KB3G [16], ZBM2 [17], GXPF1 [18] and a new revised version GXPF1A [19], which have described well the spectroscopic properties in the Ca chain. However, as pointed out in Ref. [20], "microscopic theoretical calculations with two-nucleon (NN) forces reproduce the standard magic numbers $N = 2, 8, 20$, but fail to predict ^{48}Ca as a doubly magic nucleus, making $N = 28$ the first standard magic number not reproduced in microscopic theories with two-nucleon forces". In the last few years, it has been noticed that this was mainly due to the three body forces not being included. Therefore, the interactions including NN and three-nucleon (3N) forces derived from chiral effective field theory have been developed to explain the $N = 28$ magic number [20]. Recently, calculations made with NN+3N interaction have been compared with experimental nuclear moments of $^{41-51}$Ca isotopes [10]. It turns out that, for $N \geq 27$, the calculations made with the NN+3N have an excellent agreement with the experimental magnetic and quadrupole moments. The experimental information of Sc isotopes up to and beyond $N = 28$, with one proton added to the Ca core, will be an important test for further developments of microscopic interactions.

Therefore, we propose to perform the measurement of nuclear moments and charge radii of $^{47-51}$Sc, crossing the $N = 28$ shell closure. The known information on nuclear spins, magnetic moments and quadrupole moments of Sc isotopes, measured by various experiments, are summarized in Table 1 [15, 21-27].

The single particle magnetic moment (also called the Schmidt moment) for a valence nucleon in an orbital with angular momentum j and orbital momentum l, can be estimated using the expression $\mu = (g_l l + g_s s)\mu_N$ where g_s and g_l are the spin and orbital g factors, respectively. For isotopes having a single odd nucleon outside a double-magic core (doubly magic +1), such as ^{41}Sc and ^{49}Sc, the experimental magnetic moment is found to be very close to the Schmidt moment, as deviations due to configura-

Table 1: Available information for the $^{41,44-52}$Sc isotopes. CLS refers to Collinear Laser Spectroscopy, and NMR refers to Nuclear magnetic resonance. μ and Q_s values from Refs. [23,24] are used as a reference in Ref. [15] to deduce the magnetic and quadrupole moments of $^{43-46}$Sc.

odd-even				
Isotopes	spins	μ (μ_N)	Q_s(b)	Comments
^{41}Sc	7/2-	5.431(2) [21]	(-)0.156 (3) [22]	NMR
^{43}Sc	7/2-	+4.528(10) [15]	-0.27(5) [15]	CLS
^{45}Sc	7/2-	+4.756487(2) [23]	-0.220(2) [24]	Reference in Ref.[15]
			-0.236(2)[22]	NMR
^{45m}Sc	3/2+	+0.360(11) [15]	+0.28(5) [15]	CLS
^{47}Sc	7/2-	5.33(2) [25]	-0.22(3)[25]	atomic-beam MR
^{49}Sc	7/2-	5.616(25) [26]	—	NMR
^{51}Sc	(7/2-)	—	—	—
odd-odd				
^{44}Sc	2+	+2.499(5) [15]	+0.16(4) [15]	CLS
^{44m}Sc	6+	+3.833(12) [15]	-0.21(9) [15]	CLS
^{46}Sc	4+	+3.042(8) [15]	+0.12(2) [15]	CLS
^{46m}Sc	1-	—	—	—
^{48}Sc	6+	3.785(12) [27]	—	NMR
^{50}Sc	5+	—	—	—
^{50m}Sc	(2+,3+)	—	—	—
^{52}Sc	(3+)	—	—	—

tion mixing are minimal. This is illustrated by the dashed line in the upper panel of Fig. 1.

The known experimental magnetic and quadrupole moments of Sc isotopes are plotted in Fig. 1, where they are compared with different shell-model calculations using the GXPF1A [19] and KB3G [16] effective interactions, as well as shell model calculations presented in Ref. [28]. The magnetic moments are obtained with effective single-particle $g-$factors ($g_s^{eff} = 0.9 g_s^{free}$), as shown in the upper panel of Fig. 1. The quadrupole moments (lower panel of Fig. 1) are calculated using effective charges ($e_\pi = +1.486, e_\nu = +0.840$), which were proposed in Ref. [28]. All three interactions use ^{40}Ca as the core and the pf shell as the model space for protons and neutrons, and they all predict a similar trend in the nuclear moments towards $N = 28$. Experimentally, the magnetic moment of ^{49}Sc is closer to the Schmidt value than predicted by all these calculations. For the quadrupole moments, few data are available and their error bars are too large to make firm conclusions. Thus we propose to re-measure the hyperfine spectra of all odd-Sc isotopes using a transition that is more sensitive to the quadrupole moment, and we propose to extend the earlier studies up to ^{51}Sc, which will give us magnetic and quadrupole moments across the $N = 28$ shell gap, allowing to probe its magicity.

Figure 2 shows the root mean-square (RMS) charge radii in this mass region, including recent results on K [12,29], Ca [11] and Sc isotopes [15] from bunched-beam collinear laser spectroscopy experiments using fluorescence detection. The data for Ar and Ti isotopes are taken from Ref. [30,31]. The charge radii in the Ca chain, between $N = 20$ and $N = 28$, are characterized by a parabolic shape with a large odd-even

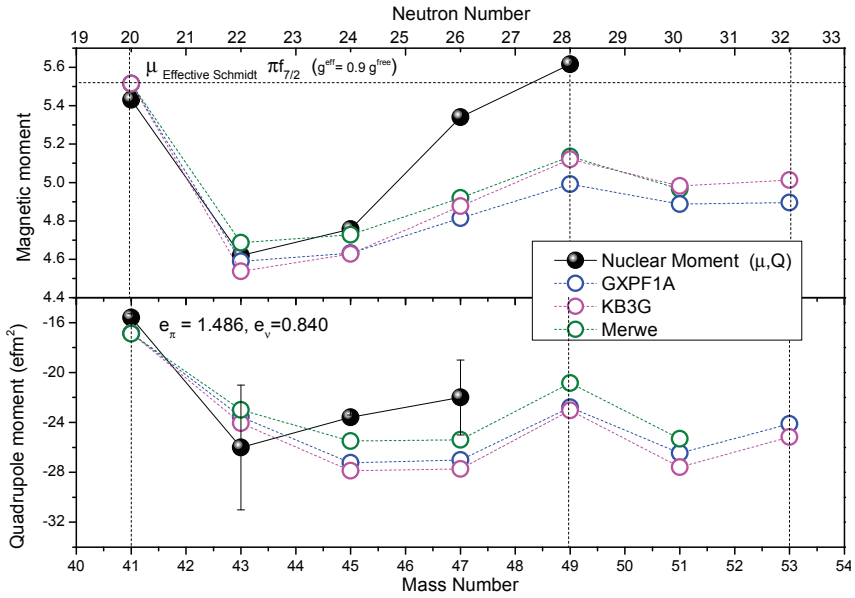

Figure 1: Experimental magnetic moments, taken from Refs. [15,21,23,25,26], compared with shell-model calculations using GXPF1A and KB3G interaction, the calculations from Merwe et al in Ref. [28], and effective Schmidt value, using effective $g-$factor ($g_s^{eff} = 0.9 g_s^{free}$)(upper panel of Figure). Experimental quadrupole moments, taken from Refs. [15,22,24,25], are compared with shell-model calculations using GXPF1A and KB3G interaction and the calculations of Ref. [28], using effective charges ($e_\pi = +1.486, e_\nu = +0.840$) which is used in Ref. [28] (lower panel).

staggering. Such a parabolic shape is much less pronounced in the K and Ar isotopes, with respectively one and two proton holes with respect to $Z = 20$. For the Sc and Ti isotopes with one and two protons outside the Ca core, the trend is not clear as not sufficient data are available. Above $N = 28$, the charge radii of K and Ca, with a similarly increasing slope, show their sensitivity to the shell closure around $N = 28$.

In the case of Sc, only limited information is available and does not reach any of the shell closures ($N = 20$, 28). The RMS charge radii measurements of $^{47-51}$Sc isotopes across/beyond $N = 28$, will provide important information to advance our understanding of the nuclear structure evolution around $N = 28$, in particular to study in more detail the apparent different behaviour for isotopes with proton particles and proton holes.

The accurate description of charge radii in medium mass nuclei has been a major challenge for nuclear theory [32]. There are many theoretical approaches trying to explain the charge radii trend of isotopes in Ca region. The general trend in the Ar chain are theoretically predicted by spherical Hartree-Fock calculations with the SGII Skyrme interaction [31], while the relativistic MF calculation can reproduce the trend of charge radii in the K chain but not the mild parabolic shape between $N = 20$ and 28, nor the odd-even staggering [12]. In the Ca isotopic chain, not a single theoretical model can fully explain the abnormal characteristics of charge radii up to $N = 32$ [11]. For the Sc isotopes, the experimental charge radii of $^{42-46}$Sc [15] have been compared with theoretical calculation using the "zbm2.renorm" interaction, which reproduced the charge radii of Ca isotopes between $N = 20$ and $N = 28$ [17]. However, the overall trend of the mean square charge radii of Sc isotopes can not been produced (Fig. 7 in Ref. [15]). Ab-initio calculations

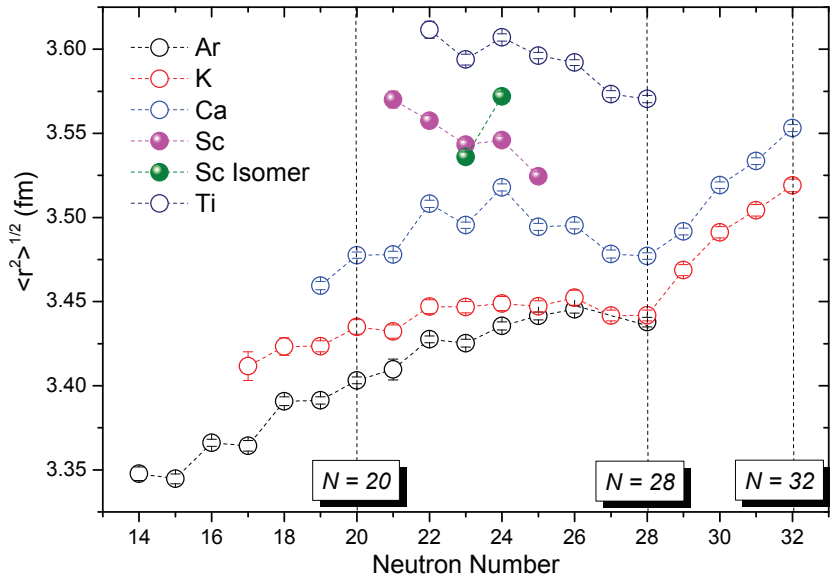

Figure 2: Root means square nuclear charge radii versus neutron number for the ground state of the K, Ca, Sc, Ar, Ti isotopes from Refs. [6,9,15,29-31].

have been successfully applied to describe binding energies and low-lying excitation spectra of Ca isotopes [33], but only up to recent, such calculations can be applied to describe charge radii of medium mass nuclei in the vicinity of doubly-magic nuclei [11,34]. As this calculation is ideally suited for nuclei with at most one or two nucleons outside a closed (sub-) shell [11], charge radii measurements of Sc isotopes, especially ^{49}Sc with doubly-magic nuclei (^{48}Ca) plus one proton, will be important for testing the Hamiltonian, and the role of many-body correlations in such ab-initio calculations [35].

2 Experimental technique

Experimental method

Using the bunched-beam collinear laser spectroscopy technique, the nuclear moments and charge radii of isotopes can be obtained by measuring their hyperfine structure. Ion beams (Sc II) will be produced from a nuclear reaction using 1.4 GeV protons impinging on a thick UCx target, and then be resonantly ionized by the Resonant Ionization Laser-Ion Source (RILIS) [36]. The extracted ion beams will be accelerated up to about $30-40$ kV and then separated by the high-resolution HRS separator. By using the ISCOOL (RFQ buncher), the ions can be cooled and bunched, and then delivered into the collinear laser spectroscopy (COLLAPS) setup, as illustrated in Fig. 3. With a fixed laser frequency which is calculated after considering the Doppler shift, the velocity of ions reaching the observation region is tuned by scanning an applied voltage until they come into resonance with the laser beam. The emitted fluorescence photons from the laser-excited atoms will be collected by four photomultiplier tubes (PMTs). Recording the counts of emitted fluorescence lights by the PMTs as a function of scanning voltage, the hyperfine structure (HFS) of the Sc isotopes can be measured. By recording the PMT signals only in a period of 5 μs, corresponding to the flight time of the bunched ion beam in front of the PMTs,

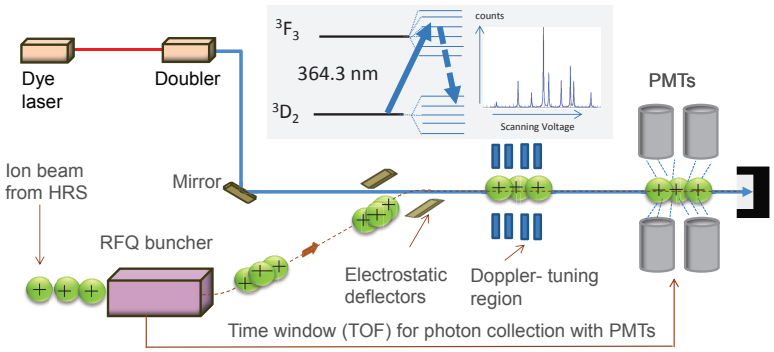

Figure 3: Schematic representation of the setup for collinear laser spectroscopy at COLLAPS [9].

the background photons from scattered laser light as well as PMT dark counts can be suppressed by a factor of 10^4 [8,10].

Spectroscopy scheme

To avoid a relatively low neutralization efficiency in the desired level after the charge exchange process and thus a low overall efficiency, the measurement will be applied to the Sc ion instead of atoms (several metastable states exist in the Sc atom, which are populated in the charge exchange process [37]). Several excitation schemes have been tested for Sc II at Jyväskylä [15]. The hyperfine A, B parameters in both the lower and upper hyperfine multiplet are also available for each scheme. To obtain a high sensitivity to the B value in both the lower and upper hyperfine multiplet and still have a relatively high efficiency, the transition from $^3D_2$ (67.72 cm^{-1}) to $^3F_3$ (27603.45 cm^{-1}) at 363.1 nm will be used, having a relatively high transition strength of 1.58×10^8 s^{-1}. Due to the low excitation energy of the $^3D_3$ and $^3D_2$ levels with respect to the $^3D_1$, all levels are well populated in the Sc ion beam. Another transition, from ground state $^3D_1$ (0 cm^{-1}) to $^3F_2$ (27443.71 cm^{-1}) at 364.3 nm, is also selected as an alternative transition with relatively high sensitivity to B value in the upper-state (transition strength: 1.521×10^8 s^{-1}). Both transitions can be accessed with a frequency-doubled narrow-band continuous-wave Ti:Sa-laser light in the 360 nm region produced using the Ti:Sapphire laser which is available at the COLLAPS laser lab. Stable beam will be requested before the experiment in order to optimize the laser/ion-beam overlap.

3 Production yields and beam time estimate

The neutron-rich radioactive Sc ion beams will be produced with a UC$_x$ target. From the ISOLDE yield database, only the yield of 13 ion/μC for ^{52}Sc is reported with 0.6

Table 2: Estimated production yield.

Isotopes	half life	yield	Target/ion source
Neutron-rich $^{50-52}$Sc			
^{50}Sc	102.5 s	$> 5 \times 10^3$	UC$_x$ /RILIS
^{51}Sc	12.4 s	$> 5 \times 10^3$	UC$_x$ /RILIS
^{52}Sc	8.2 s	$\sim 5 \times 10^3$	UC$_x$ /RILIS

GeV proton energy on a UC_x target and a tungsten surface ioniser [37]. However, the development of the ionization scheme of Sc in RILIS has demonstrated that a factor of 400 enhancement in the Sc production yield can be obtained with respect to the surface-ionized yield [39,40]. Therefore, on the basis of the ISOLDE yield database and the development of ionization scheme of Sc with RILIS, the production yield for the neutron-rich Sc can be estimated as listed in Table 2 [11] . However, due to the uncertainty of the estimated yield and that the radioactive Sc isotopes were not produced during ISOLTRAP run in 2014, a yield check prior to scheduling the experiment will be requested.

For the experiments with the COLLAPS setup, the general limitation for the yield of studied isotopes is several 1000 ions/s. The minimum amount of ions needed for an experiment depends on the hyperfine transition that is studied (its oscillator strength and its electronic configurations), but also on the efficiency in populating the atomic or ionic level from which the resonant excitation takes place. For example, the sensitivity reached a few 100 ions/s in past experiments on Ca and Cd, in which ions were laser excited instead of atoms (thus limiting losses in the charge exchange process). In the particular case of Sc II, where 3 low-lying states are populated in the ion beam and thus the population from which the resonant excitation starts, is reduced by at least a factor of 3, we expect to reach easily ^{51}Sc. In order to determine charge radii from isotope shift measurements, each hyperfine spectrum has to be measured relative to that of a reference isotope hyperfine spectrum. Therefore, we count 1 shift for each set of two isotopes (new and reference), considering that several hyperfine scans are taken in order to reduce statistical and systematic errors.

Therefore, to study the neutron-rich isotopes and isomers between ^{45}Sc (ref.) and ^{51}Sc (7 isotopes and 3 isomers, of which 6 will be measured for the first time), we request a total of 12 shifts, and an additional 2 shifts with stable beam prior to the run for optimizing the experimental set-up and laser transitions for optimum efficiency.

Beyond ^{51}Sc, the production yields will be too low for COLLAPS, but are still accessible using the CRIS experiment and single-ion detection. Therefore a second proposal for an experiment at CRIS in order to study the more exotic isotopes is submitted parallel to this proposal.

Summary of requested shifts: 12 shifts of radioactive beam time and 2 shifts of stable beam are requested.

References

[1] L. Coraggio et al., Phys. Rev. C **80**, 044311 (2009)
[2] Ning Wang and Tao Li., Phys. Rev. C **88**, 011301(R)(2013)
[3] Y. Utsuno et al., JPS Conf. Proc. **6**, 010007 (2015).
[4] D. Steppenbeck et al., Nature 502, 207 (2013).
[5] F. Wienholtz et al., Nature 498, 346 (2013).

[6] S. N. Liddick et al., Phys. Rev. C **70**, 064303 (2004).
[7] H. L. Crawford et al., Phys. Rev. C ^{82}, 014311 (2010).
[8] J. Papuga et al., Phys. Rev. Lett. **110**, 172503 (2013)
[9] J. Papuga et al., Phys. Rev. C **90**, 034321 (2014).
[10] R. F. Garcia Ruiz et al., Phys. Rev. C **91**, 041304(R) (2015).
[11] R. F Garcia Ruiz et al. Submitted to Nature Physics (2015).
[12] K. Kreim et al., Phys. Lett. B **73** 197 (2014).
[13] M. Rosenbusch et al.,Phys. Rev. Lett. **114**, 202501 (2015).
[14] D. Beck et al., "Seeking the Purported Magic Number $N = 32$ with High-Precision Mass Spectrometry",INTC IS532 (2014).
[15] M. Avgoulea et al., J. Phys. G: Nucl. Part. Phys. **38**, 025104 (2011).
[16] A. Poves et al., Nucl. Phys. A **694**, 157 (2001).
[17] E. Caurier et al., Phys. Lett. B 522, 240 (2001).
[18] M. Honma et al., Phys. Rev. C **65**, 061301(R) (2002).
[19] M. Honma et al., Eur. Phys. J. A **25**, s01, 499502 (2005).
[20] Jason D Holt et al., J. Phys. G: Nucl. Part. Phys. **39** 085111 (2012).
[21] T. Minamisono et al., Nucl.Phys. A **516**, 365 (1990);
[22] T. Minamisono et al., Z. Naturforsch. A **57**, 595 (2002).
[23] O. Lutz, Phys. Lett. A **29**, 58 (1969).
[24] V. Kellö et al., Chemical Physics Letters **329**, 112 (2000)
[25] R. G. Cornwell et al., Phys. Rev. **141**, 1106 (1966).
[26] T. Ohtsubo et al., Phys. Rev. lett. **109**, 032504 (2012).
[27] T. Ohtsubo et al., Hyperfine Interact **180**, 79 (2007).
[28] M.G. van der Merwe et al., Nuclear Physics A **579**, 173-196 (1994).
[29] D. M. Rossi et al., phys. Rev. C **92**, 014305 (2015).
[30] I. Angeli, K.P. Marinova., Atomic Data and Nuclear Data Tables **99** 69 (2013).
[31] K. Blaum et al., Nucl. Phys. A **799**, 30 (2008)
[32] A. Ekström et al., Phys. Rev. C **91**, 051301(R) (2015).
[33] G. Hagen et al., Phys. Rev. lett **109**, 032502 (2012).
[34] G. Hagen et al (accepted in Nature physics) (2015).
[35] G. Hagen (Private communication).
[36] V. Fedosseev et al., Nucl. Instrum. Methods Phys. Res., Sect. B **204**, 353 (2003).
[37] K. Minamisono (Private communication).
[38] H.-J. Kluge, CERN 86-05 (1986).
[39] R. Catherall, et al., Rev. Sci. Instr. **75**, 1614 (2004).
[40] V. N. Fedosseev et al., Hyp. Int. **162**, 15 (2005).

Appendix

DESCRIPTION OF THE PROPOSED EXPERIMENT
The experimental setup comprises: COLLAPS

Part of the	Availability	Design and manufacturing
(COLLAPS)	☒ Existing	☒ To be used without any modification

HAZARDS GENERATED BY THE EXPERIMENT
Hazards named in the document relevant for the fixed CRIS installation.

Additional hazards: None